

# Binuclear iridium complexes containing bridging 1,2-dicarba-closo-dodecaborane-1,2-dichalcogenolato ligands: Molecular structures of the complexes $[(\text{CODIr})_2(\mu_2\text{-S}_2\text{C}_2(\text{B}_{10}\text{H}_{10}))]$ and $[(\text{Cp}^*\text{Ir})_2(\mu_2\text{-Se}_2\text{C}_2(\text{B}_{10}\text{H}_{10}))]$

Yin-Qiang Chen, Jian-Qiang Wang, Guo-Xin Jin \*

Shanghai Key Laboratory of Molecular Catalysis and Innovative Material, Department of Chemistry, Fudan University, Shanghai 200433, China

Received 14 June 2007; received in revised form 29 July 2007; accepted 31 July 2007  
Available online 6 August 2007

## Abstract

Four binuclear iridium complexes with a chelating 1,2-dicarba-closo-dodecaborane-1,2-dichalcogenolato ligands  $[\text{Ir}_2(\text{COD})_2(\mu_2\text{-E}_2\text{C}_2\text{B}_{10}\text{H}_{10})]$  [E = S (**3a**), Se (**3b**)]  $[(\text{Cp}^*\text{Ir})_2(\mu_2\text{-E}_2\text{C}_2\text{B}_{10}\text{H}_{10})]$  [E = S (**5a**), Se (**5b**)] have been synthesized through different method. The formal oxidation state of iridium in complexes **3** and **5** are I and II, respectively, due to the different electron donor coordinated to the iridium center. All four complexes **3a–5b** are characterized by IR,  $^1\text{H}$ ,  $^{13}\text{C}$ ,  $^{11}\text{B}$  NMR spectra and elemental analyses. The molecular structures of complex **3a** and **5b** have been determined by X-ray crystallographic analysis, only **5b** shows the metal–metal interaction between the two iridium atoms.

© 2007 Elsevier B.V. All rights reserved.

**Keywords:** Iridium; Binuclear; Dichalcogenolato ligands; Carborane; Molecular structures

## 1. Introduction

Recently, much attention has focused on the chemistry of multinuclear transition-metal complexes [1]. The expected cooperation between metal atoms to perform novel chemical transformations is the basic idea that promotes most of the research in binuclear complexes [2]. Such cooperation can be the consequence of an overall change in the reactivity due to the proximity of both metals; such examples can be found in the chemistry of binuclear iridium compounds, which very frequently give rise to complexes in oxidation state II. Whilst the activation of molecules such as halogens or halocarbons by diiridium(I) complexes has been extensively documented [3] and numerous other applications for the dinuclear iridium complexes have been introduced recently [4].

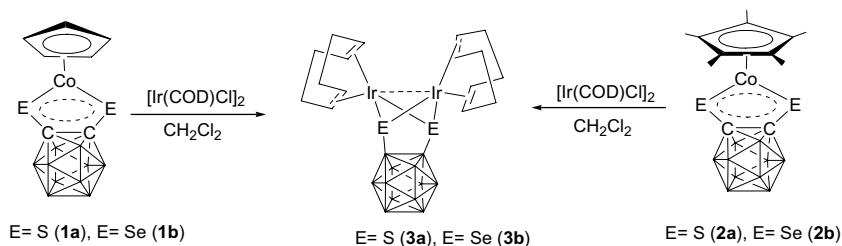
We report here the synthesis and the characterization of two types of dinuclear iridium carborane complexes, **3a**, **b** and **5a**, **b**. The hemisphere of the iridium atom is shielded by cyclooctadiene group or the  $\text{Cp}^*$  ligand in complexes **3** or **5**, respectively, which causes different electronic environment around the iridium center and the oxidation state of iridium in **3** and **5** are +I [5] and +II, respectively.

## 2. Results and discussion

### 2.1. Syntheses of complexes **3a**, **b** and **5a**, **b**

The 16 electron half-sandwich cobalt complexes  $[\text{Cp}'\text{CoE}_2\text{C}_2(\text{B}_{10}\text{H}_{10})]$  [ $\text{Cp}' = \eta^5\text{-C}_5\text{H}_5$ , E = S (**1a**), E = Se (**1b**);  $\text{Cp}' = \eta^5\text{-C}_5(\text{CH}_3)_5$ , E = S (**2a**), E = Se (**2b**)] [6] were used in the synthesis of **3a** and **3b**. After these four starting compounds react with  $[\text{Ir}(\text{COD})\text{Cl}]_2$  in dichloromethane respectively, diiridium complex **3a** or **3b** in the formula of  $[\text{Ir}_2(\text{COD})_2(\mu_2\text{-E}_2\text{C}_2\text{B}_{10}\text{H}_{10})]$  is the only product after separation (Scheme 1). It is interesting to notice that in

\* Corresponding author. Tel.: +86 21 65643776; fax: +86 21 65641740.  
E-mail address: [gxjin@fudan.edu.cn](mailto:gxjin@fudan.edu.cn) (G.-X. Jin).

Scheme 1. Synthesis of **3a** and **3b**.

our previous work, through using different low valent transition-metal carbonyl or COD complexes we synthesized numerous multinuclear cobalt carborane complexes [7], but in the case of  $[\text{Ir}(\text{COD})\text{Cl}]_2$  or  $[\text{Rh}(\text{COD})\text{Cl}]_2$  only homodinuclear species can be obtained. Furthermore, different solvents and reacting conditions were introduced into this reaction, but complex **3a** or **3b** is the only product. This is in agreement with the reactions of **1a–2b** with  $[\text{Rh}(\text{COD})\text{Cl}]_2$  [7].

Complexes **3a** and **3b** can be obtained in good yields as blue crystals, which are slightly air and moisture sensitive in the solvent and stable in the solid state for a couple of days, soluble even in hexane.

Complexes **5a** or **5b** can be synthesized directly by the reaction of  $[\text{Cp}^*\text{IrCl}(\mu\text{-Cl})_2]$  with **4a** or **4b** in low yields (Scheme 2) (1–2%), and the mononuclear 16electron half-sandwich iridium complexes  $\text{Cp}^*\text{IrE}_2\text{C}_2(\text{B}_{10}\text{H}_{10})$  [E = S (**6a**), Se (**6b**)] have been isolated as the main products in the reactions [8]. Complexes **5a** and **5b** are red crystals and are quite stable both in solid state and solution. In the formation of all the Co, Rh, Ir dinuclear half-sandwich complexes  $[(\text{Cp}^*\text{M})_2\text{E}_2\text{C}_2\text{B}_{10}\text{H}_{10}]$ , the yields of the dinuclear iridium complexes are relatively lower. That's partly because iridium has the lowest oxidisability, and it is difficult for the  $\text{Ir}^{3+}$  to turn into the  $\text{Ir}^{2+}$  form, while the yields of the cobalt dinuclear half-sandwich carborane complexes are the highest.

The NMR and Ir spectroscopy data of complexes **3a** and **3b** are in agreement with the structure we obtained from the X-ray crystallography. The  $^1\text{H}$  NMR spectrum of **3a** shows clearly the resonance of the methylene groups of the cyclooctadiene ligand at  $\delta$  1.92, 2.01, 2.29 and 2.33 ppm as multiplets, and signals for olefin protons at  $\delta$  3.65 and 4.44 ppm. There are two sets of  $^1\text{H}$  NMR signals for the cyclooctadiene moiety, which indicates that the two

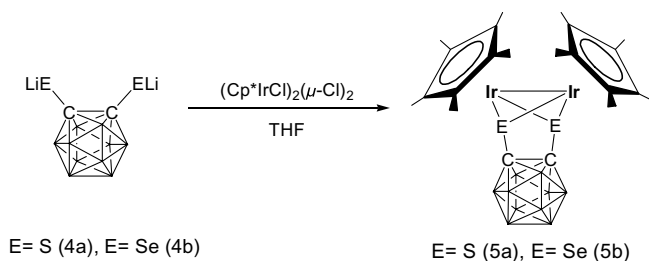
COD ligands are in the different chemical environments, and the structure is not symmetric [5]. In the  $^{13}\text{C}$  spectrum there are two signals for the olefin protons at  $\delta$  67.3 and 65.4 ppm, and the carbon atoms of the carborane moiety give rise to a singlet at  $\delta$  87.6 ppm. In the higher field there are two singlets at  $\delta$  32.5 and 32.4 ppm for the carbon atoms of the methylene group. The IR spectrum is also in good agreement with the results, typical B–H vibration signal at  $2582\text{ cm}^{-1}$ , and one  $\nu(\text{C}=\text{C})$  stretching around  $1631\text{ cm}^{-1}$ . Complex **3b** has the similar structure with complex **3a**, thus the spectrum data are basically the same, except for a  $^{13}\text{C}$  NMR resonance at  $\delta$  67.4 ppm for the C–Se moiety.

Complexes **5a** and **5b** also have the half-sandwich dinuclear structure, but the spectrum data are quite simple compared to the **3a** and **3b**. The NMR and IR spectroscopic data are in agreement with the structure. **5a** and **5b** clearly have  $^1\text{H}$  and  $^{13}\text{C}$  NMR resonance for the  $\text{CH}_3$  group in the  $\text{Cp}^*$  moiety at  $\delta$  1.83, 1.89 and 10.1, 11.2 ppm respectively. The  $^{13}\text{C}$  NMR signals for the carbon atoms belong to the carborane moiety in **5a** and **5b** are at  $\delta$  92.8 and 77.2 ppm respectively. In the IR spectrum, the B–H stretching is clearly observed at  $2586$  and  $2587\text{ cm}^{-1}$  for **5a** and **5b**.

## 2.2. Molecular structure

The molecular structures of  $[(\text{CODIr})_2(\mu_2\text{-S}_2\text{C}_2\text{-}(\text{B}_{10}\text{H}_{10}))]$  **3a** and  $(\text{Cp}^*\text{Ir})_2[\mu_2\text{-Se}_2\text{C}_2(\text{B}_{10}\text{H}_{10})]$  **5b** were determined by single crystal X-ray diffraction. Suitable crystal was obtained by slow diffusion of hexane into a dichloromethane solution at low temperature.

The X-ray structure of complex **3a** is depicted in Fig. 1, it is an iridium (I) thiolate dimer. Dithiolato carborane serves as a bridging ligand to combine the biiridium center, and contributes three electrons to each iridium atom. Each iridium atom is further coordinated by a cyclooctadienyl ligand. The distance between the two Ir atoms is  $2.8608(11)\text{ \AA}$ , which indicates certain interaction between the two iridium atoms. The coordination geometry around each iridium atom is approximately square planar. The  $\text{Ir}_2\text{S}_2$  ring is highly puckered, the dihedral angle between the planes  $\text{Ir1Ir2S1}$  and  $\text{Ir1Ir2S2}$  is  $107.627(15)^\circ$ . The bond length of Ir–S varies from  $2.389(4)$  to  $2.416(4)\text{ \AA}$ , which is in the longer range of that found for binuclear thiolate-bridged complexes [7]. The Ir–C bond distances fall in

Scheme 2. Synthesis of **5a** and **5b**.

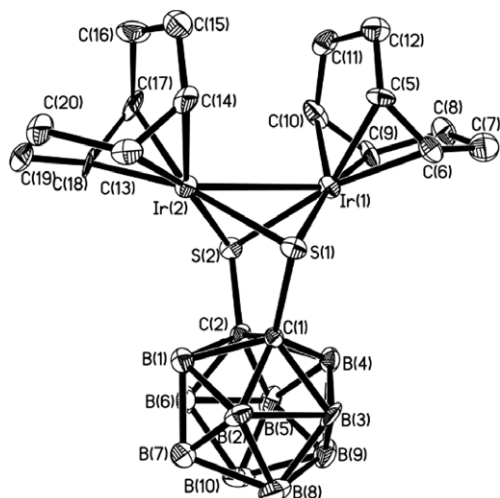


Fig. 1. Molecular structure of complex **3a**. Selected distances (Å) and angles (°): Ir(1)–Ir(2), 2.8608(11); Ir(1)–S(1), 2.389(4); Ir(1)–S(2), 2.401(4); Ir(1)–C(5), 2.127(16); Ir(1)–C(6), 2.096(16); Ir(1)–C(9), 2.121(17); Ir(1)–C(10), 2.130(16); C(5)–Ir(1)–C(6) 37.8(6); C(9)–Ir(1)–C(10) 37.9(7); Ir(2)–Ir(1)–S(1), 53.06(10); Ir(1)–S(1)–Ir(2), 73.15(11); C(5)–Ir(1)–S(1), 93.7(5).

the range of 2.096(16) to 2.160(17) Å, which is normal for Ir complexes containing COD ligands *trans* to S donor atoms [9].

The structure of complex **5b** is also solved, and it is shown in Fig. 2. It is a binuclear iridium complex as **3a**, the distance between Ir(1) and Ir(2) is 2.6924(8) Å which indicates a single metal–metal bond nature. Each iridium is coordinated by one Cp\* ligand, single bonded to the other iridium atom, and bridged by two  $\mu_3$ -Se atoms from the diselenolate carborane moiety. Both of the iridium (II) centers adopt a three-legged piano-stool conformation and have a six-coordinated geometry. The distances between iridium and selenium atoms are around 2.4300 Å which fall

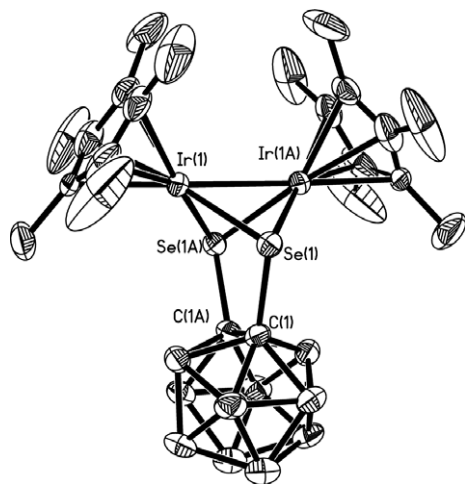


Fig. 2. Molecular structure of complex **5b**. Symmetry transformations used to generate equivalent atoms:  $-x + 1, y, -z + 1/2$ . Selected distances (Å) and angles (°): Ir(1)–Ir(2), 2.6924(8); Ir(1)–Se(1), 2.4361(8); Ir(1)–Se(1A), 2.4274(8); Ir(1)–Ir(1A)–Se(1), 56.23(2); Ir(1)–Se(1)–Ir(1A), 67.23(2); Se(1)–Ir(1)–Se(1A), 81.40(3).

in the normal single Ir–Se bond range, but longer than that of the monomer (Cp\*IrSe<sub>2</sub>C<sub>2</sub>B<sub>10</sub>H<sub>10</sub>) which is around 2.3600 Å. The bond length of Ir–C varies from 2.158(8) to 2.217(8) Å. The Ir<sub>2</sub>S<sub>2</sub> ring is also highly puckered, the dihedral angle between the planes Ir1Ir1ASe1 and Ir1Ir1A–Se1A is 103.073(2)°.

### 3. Experimental

All manipulations were performed under an atmosphere of nitrogen using standard Schlenk techniques. Solvents were dried by refluxing over sodium/benzophenone ketyl (toluene, hexane, THF, diethyl ether) and distilled just before use. And dichloromethane was dried and distilled over CaH<sub>2</sub>. The [Ir(COD)Cl]<sub>2</sub> [10] and Li<sub>2</sub>C<sub>2</sub>E<sub>2</sub>B<sub>10</sub>H<sub>10</sub> [E = S (**4a**), Se (**4b**)] [11] were synthesized via the literature procedure. IrCl<sub>3</sub>nH<sub>2</sub>O were used as purchased. IR spectra were recorded on a Nicolet AVATAR-360 IR spectrometer, whereas <sup>1</sup>H (500 MHz), <sup>11</sup>B (160 MHz), and <sup>13</sup>C (125 MHz) NMR spectra were obtained on a Bruker DMX-500 spectrophotometer in CDCl<sub>3</sub> solution. Elemental analyses were performed on an Elementar III Vario EI analyzer.

#### 3.1. [Ir<sub>2</sub>(COD)<sub>2</sub>(μ<sub>2</sub>-E<sub>2</sub>C<sub>2</sub>B<sub>10</sub>H<sub>10</sub>)] [E = S (**3a**), Se (**3b**)]

To a solution of **1a** (66 mg, 0.2 mmol) or **1b** (84 mg, 0.2 mmol) in 20 ml dichloromethane was added [Ir(COD)Cl]<sub>2</sub> (134 mg, 0.2 mmol). The suspension was stirred for 3 h at room temperature. The solvent was removed under vacuum. The residue was dissolved in 3 mL of dichloromethane and chromatographed on silica gel to afford **3a** (132 mg, 81%) and **3b** (135 mg, 75%) as blue solids. Recrystallization of **3a** from CH<sub>2</sub>Cl<sub>2</sub>/hexane afforded dark blue crystals. Complex **3a**: Anal. Calc. for C<sub>18</sub>H<sub>34</sub>Ir<sub>2</sub>S<sub>2</sub>B<sub>10</sub>: C, 26.79; H, 4.25. Found: C, 25.62; H, 4.41%. <sup>1</sup>H NMR (500 MHz, CDCl<sub>3</sub>, δ/ppm): δ 1.92 (m, 4H, CH<sub>2</sub>), 2.01 (m, 4H, CH<sub>2</sub>), 2.29 (m, 4H, CH<sub>2</sub>), 2.33 (m, 4H, CH<sub>2</sub>), 3.65 (m, 4H, CH), 4.44 (m, 4H, CH). <sup>11</sup>B NMR (160 MHz, CDCl<sub>3</sub>, δ/ppm): δ 7.9, –7.1, –9.6, –11.3. <sup>13</sup>C NMR (125 MHz, CDCl<sub>3</sub>, δ/ppm): δ 87.6 (s, CS), 67.3 (s, CH), 65.4 (s, CH), 32.5 (s, CH<sub>2</sub>), 32.4 (s, CH<sub>2</sub>). IR (KBr disk cm<sup>-1</sup>): ν = 2582 (B–H); ν = 1631 (C=C). Complex **3b**: Anal. Calc. for C<sub>18</sub>H<sub>34</sub>Ir<sub>2</sub>Se<sub>2</sub>B<sub>10</sub>: C, 24.00; H, 3.80. Found: C, 25.11; H, 3.67%. <sup>1</sup>H NMR (500 MHz, CDCl<sub>3</sub>, δ/ppm): δ 1.91 (m, 4H, CH<sub>2</sub>), 2.12 (m, 4H, CH<sub>2</sub>), 2.46 (m, 4H, CH<sub>2</sub>), 2.60 (m, 4H, CH<sub>2</sub>), 4.10 (s, 4H, CH), 4.88 (m, 4H, CH). <sup>11</sup>B NMR (160 MHz, CDCl<sub>3</sub>, δ/ppm): δ 6.3, –7.7, –9.4, –10.9. <sup>13</sup>C NMR (125 MHz, CDCl<sub>3</sub>, δ/ppm): δ 78.4 (s, CH), 78.2 (s, CH), 67.4 (s, CSe), 33.2 (s, CH<sub>2</sub>), 32.7 (s, CH<sub>2</sub>). IR (KBr disk cm<sup>-1</sup>): ν = 2578 (B–H); ν = 1633 (C=C).

#### 3.2. [(Cp\*Ir)<sub>2</sub>(μ<sub>2</sub>-E<sub>2</sub>C<sub>2</sub>B<sub>10</sub>H<sub>10</sub>)] [E = S (**5a**), Se (**5b**)]

To a solution of **4a** (1 mmol) or **4b** (1 mmol) in 40 mL ether was added (Cp\*IrCl)<sub>2</sub>(μ<sub>2</sub>-Cl)<sub>2</sub> (400 mg, 1 mmol)

followed by 30 mL of THF. The suspension was stirred for 12 h at room temperature. The solvent was removed under vacuum. Then the residue was dissolved in 3 mL of dichloromethane and chromatographed on silica gel to afford **5a** (17 mg, 2%), **5b** (10 mg, 1%) as red solids and **6a** (448 mg, 84%), **6b** (565 mg, 90%) as blue products. Recrystallization of **5b** from CH<sub>2</sub>Cl<sub>2</sub>/hexane afforded red crystals. Complex **5a**: Anal. Calc. for C<sub>22</sub>H<sub>40</sub>Ir<sub>2</sub>S<sub>2</sub>B<sub>10</sub>: C, 30.32; H, 4.63. Found: C, 30.68; H, 4.68%. <sup>1</sup>H NMR (500 MHz, CDCl<sub>3</sub>, δ/ppm): δ 1.83 (s, 30H, CH<sub>3</sub>). <sup>11</sup>B NMR (160 MHz, CDCl<sub>3</sub>, δ/ppm): δ -4.3, -6.9, -8.3, -10.7. <sup>13</sup>C NMR (125 MHz, CDCl<sub>3</sub>, δ/ppm): δ 10.1 (s, CH<sub>3</sub>), 91.8 (s, C<sub>5</sub>(CH<sub>3</sub>)<sub>5</sub>), 92.8 (s, CS). IR (KBr disk cm<sup>-1</sup>): ν = 2586 (B–H). Complex **5b**: Anal. Calc. for C<sub>22</sub>H<sub>40</sub>Ir<sub>2</sub>Se<sub>2</sub>B<sub>10</sub>: C, 27.67; H, 4.22. Found: C, 27.36; H, 4.12. <sup>1</sup>H NMR (500 MHz, CDCl<sub>3</sub>, δ/ppm): δ 1.89 (s, 30H, CH<sub>3</sub>). <sup>11</sup>B NMR (160 MHz, CDCl<sub>3</sub>, δ/ppm): δ -5.3, -7.3, -8.5, -11.2. <sup>13</sup>C NMR (125 MHz, CDCl<sub>3</sub>, δ/ppm): δ 11.2 (s, CH<sub>3</sub>), 77.2 (s, CSe), 88.4 (s, C<sub>5</sub>(CH<sub>3</sub>)<sub>5</sub>). IR (KBr disk cm<sup>-1</sup>): ν = 2587 (B–H). Complex **6a**: Anal. Calc. for C<sub>12</sub>H<sub>25</sub>IrS<sub>2</sub>B<sub>10</sub>: C, 27.00; H, 4.72. Found: C, 26.76; H, 4.70%. <sup>1</sup>H NMR (500 MHz, CDCl<sub>3</sub>, δ/ppm): δ 1.86 (s, 15H, CH<sub>3</sub>). <sup>11</sup>B NMR (160 MHz, CDCl<sub>3</sub>, δ/ppm): δ -5.4, -7.0, -7.8, -9.6, -11.1. <sup>13</sup>C NMR (125 MHz, CDCl<sub>3</sub>, δ/ppm): δ 10.09 (s, CH<sub>3</sub>), 91.82 (s, C<sub>5</sub>(CH<sub>3</sub>)<sub>5</sub>), 92.83 (s, CS). IR (KBr disk cm<sup>-1</sup>): ν = 2959, 2920 (C–H), 2597 (B–H). Complex **6b**: Anal. Calc. for C<sub>12</sub>H<sub>25</sub>IrSe<sub>2</sub>B<sub>10</sub>: C, 25.63; H, 4.48. Found: C, 25.56; H, 4.42. <sup>1</sup>H NMR (500 MHz, CDCl<sub>3</sub>, δ/ppm): δ 1.90 (s, 15H, CH<sub>3</sub>). IR (KBr disk cm<sup>-1</sup>): ν = 2577 (B–H).

### 3.3. X-ray crystal structure analysis

Single crystal was sealed in glass capillaries and was sequentially mounted on CCD-Bruker smart diffractometer. The determinations of unit and intensity data were performed with graphite monochromated Mo Kα radiation (λ = 0.71073 Å). All the data were collected at room temperature using the scan technique. The structure was solved by the direct methods expanded using Fourier techniques and refined on F<sup>2</sup> by a full-matrix least-squares method. The non-hydrogen atoms were refined anisotropically and hydrogen atoms were included but not refined. Details of crystal data for **3a** and **5b** are summarized in Table 1.

Crystallography data (excluding structure factors) for the structures reported in this paper have been deposited with the Cambridge Crystallographic Data Center, CCDC. Copies of these data can be obtained free of charge on application to the Director, CCDC, 12 Union Road, Cambridge CB2 1EZ, UK (fax: +44-1223-336033; e-mail: deposit@ccdc.ac.uk or <http://www.http.ccdc.cam.ac.uk>).

### 5. Supplementary material

CCDC 650342 and 650343 contain the supplementary crystallographic data for **3a** and **5b**. These data can be obtained free of charge via <http://www.ccdc.cam.ac.uk/conts/retrieving.html>, or from the Cambridge Crystallographic Data Centre, 12 Union Road, Cambridge CB2

Table 1  
X-ray crystallographic data and processing parameters for **3a** and **5b**

	3a	5b
Empirical formula	C <sub>18</sub> H <sub>34</sub> Ir <sub>2</sub> S <sub>2</sub> B <sub>10</sub>	C <sub>22</sub> H <sub>40</sub> Ir <sub>2</sub> Se <sub>2</sub> B <sub>10</sub>
Formula weight	807.07	955.02
Crystal system	Triclinic	Monoclinic
Space group	P1	C2/c
<i>Unit cell dimensions</i>		
<i>a</i> (Å)	12.677(4)	18.275(5)
<i>b</i> (Å)	12.744(4)	12.562(3)
<i>c</i> (Å)	16.909(5)	15.242(4)
<i>α</i> (°)	104.500(4)	90
<i>β</i> (°)	104.072(4)	114.255(3)
<i>γ</i> (°)	97.901(4)	90
Volume (Å <sup>3</sup> )	1302.2(6)	3190.1(14)
<i>Z</i>	4	8
Absorption coefficient (mm <sup>-1</sup> )	6.172	10.628
Crystal size (mm)	0.20 × 0.15 × 0.10	0.20 × 0.15 × 0.10
Calculated density (mg/m <sup>3</sup> )	2.138	1.988
<i>F</i> (000)	1512	1776
<i>θ</i> Range (°)	1.30–27.16	2.03–27.12
<i>h</i> , <i>k</i> , <i>l</i> collected	–14, 16, –16, 10, ±21	–23, 19, –16, 10, –17, 19
Reflections collected/unique [ <i>R</i> (int)]	12619/10641 [0.0673]	7785/3492 [0.0312]
Data/restraints/parameters	10641/0/597	3492/0/168
Goodness-of-fit <sup>a</sup> on <i>F</i> <sup>2</sup>	0.899	0.974
Final <i>R</i> indices [ <i>I</i> > 2σ( <i>I</i> )] <sup>b</sup>	<i>R</i> <sub>1</sub> = 0.0574, <i>wR</i> <sub>2</sub> = 0.1281	<i>R</i> <sub>1</sub> = 0.0340, <i>wR</i> <sub>2</sub> = 0.0822
<i>R</i> indices (all data)	<i>R</i> <sub>1</sub> = 0.0989, <i>wR</i> <sub>2</sub> = 0.1594	<i>R</i> <sub>1</sub> = 0.0525, <i>wR</i> <sub>2</sub> = 0.0955
Largest difference peak and hole (e Å <sup>-3</sup> )	3.225 and –4.319	1.788 and –1.434

<sup>a</sup>  $S = [\sum(w(F_o^2 - F_c^2))^2 / (n - p)]^{1/2}$ .

<sup>b</sup>  $R_1 = \sum|F_o| - |F_c| / \sum|F_o|$ ;  $R_w = [\sum w(|F_o^2| - |F_c^2|)_2 / \sum w|F_o^2|]^{1/2}$ .

1EZ, UK, fax: (+44) 1223-336-033, or e-mail: deposit@ccdc.cam.ac.uk.

### Acknowledgements

Financial support by the National Science Foundation of China for Distinguished Young Scholars (20531020, 20421303), by the National Basic Research Program of China (2005CB623800) and by Shanghai Science and Technology Committee (05JC14003, 06XD14002) is gratefully acknowledged.

### References

- [1] (a) A.F. Heyduk, D.G. Nocera, *Chem. Commun.* (1999) 1519;  
(b) T. Iwasa, H. Shimada, A. Takami, H. Matsuzaka, Y. Ishii, M. Hidai, *Inorg. Chem.* 38 (1999) 2851;  
(c) M.V. Jiménez, E. Sola, A.P. Martinez, F.J. Lahoz, L.A. Oro, *Organometallics* 18 (1999) 1125;  
(d) D.A. Vacic, W.D. Jones, *Organometallics* 18 (1999) 134;  
(e) K. Tani, A. Iseki, T. Yamagata, *Angew. Chem., Int. Ed.* 37 (1998) 3381;  
(f) M.A. Arthurs, J. Bickerton, S.R. Stobart, J. Wang, *Organometallics* 17 (1998) 2743;  
(g) H. Matsuzaka, K. Ariga, H. Kase, T. Kamura, M. Kondo, S. Kitagawa, M. Yamasaki, *Organometallics* 16 (1997) 4514;  
(h) D.M. Heinekey, D.A. Fine, D. Barnhart, *Organometallics* 16 (1997) 2530;  
(i) Z. Tang, Y. Nomura, Y. Ishii, Y. Mizobe, M. Hidai, *Organometallics* 16 (1997) 151.
- [2] (a) Y. Takagi, H. Matsuzaka, Y. Ishii, M. Hidai, *Organometallics* 16 (1997) 4445;  
(b) K. Tada, M. Oishi, H. Suzuki, *Organometallics* 15 (1996) 2422;  
(c) H.F. Antwi-Nsiah, O. Oke, M. Cowie, *Organometallics* 15 (1996) 1042;  
(d) G. Meister, G. Rheinwald, H. Stoeckli-Evans, G. Süss-Fink, J. *Organomet. Chem.* 496 (1995) 197.
- [3] (a) C. Tejel, M.A. Ciriano, J.A. López, F.J. Lahoz, L.A. Oro, *Organometallics* 16 (1997) 4718;  
(b) M.A. Ciriano, J.J. Pérez-Torrente, L.A. Oro, *J. Organomet. Chem.* 445 (1993) 273;  
(c) G.W. Bushnell, S.R. Stobart, J. Wang, *Organometallics* 15 (1996) 3785.
- [4] (a) M.V. Jiménez, E. Sola, L.A. Oro, *Chem. Eur. J.* 4 (1998) 1398;  
(b) D.R. Petrovic, D.J. Anderson, J.R. Torkelson, R. McDonald, M. Cowie, *Organometallics* 22 (2003) 4647;  
(c) A.S. Veige, T.G. Gray, D.G. Nocera, *Inorg. Chem.* 44 (2005) 17.
- [5] S.Y. Cai, X.F. Hou, L.H. Weng, G.-X. Jin, *J. Organomet. Chem.* 690 (2005) 910.
- [6] (a) D.H. Kim, J. Ko, K. Park, S. Cho, S.O. Kang, *Organometallics* 18 (1999) 2738;  
(b) J.H. Won, D.H. Kim, B.Y. Kim, S.J. Kim, C. Lee, S. Cho, J. Ko, S.O. Kang, *Organometallics* 21 (2002) 1443;  
(c) X.-F. Hou, X.-C. Wang, G.-X. Jin, *J. Organomet. Chem.* 689 (2004) 2228.
- [7] Y.-Q. Chen, J.S. Zhang, G.-X. Jin, *Dalton Trans.* (2007) 749.
- [8] J.H. Won, D.H. Kim, B.Y. Kim, S.J. Kim, C. Lee, S. Cho, J. Ko, S.O. Kang, *Organometallics* 21 (2002) 1443.
- [9] J.Q. Wang, M. Herberhold, G.-X. Jin, *Organometallics* 25 (2006) 3508.
- [10] R.H. Crabtree, J.M. Quirk, H. Felkin, T. Fillebeen-Kahn, *Synth. React. Inorg. Met.-Org. Chem.* 12 (1982) 407.
- [11] (a) X.Y. Yu, G.-X. Jin, N.H. Hu, L.H. Weng, *Organometallics* 21 (2002) 5540;  
(b) M. Herberhold, G.-X. Jin, H. Yan, W. Milius, B. Wrackmeyer, *J. Organomet. Chem.* 587 (1999) 252.